Effects of parametric perturbations on the onset of chaos in the Josephson-junction model: Theory and analog experiments

Giampaolo Cicogna
Dipartimento di Fisica, Università di Pisa, Piazza Torricelli 2, Pisa, Italy

Leone Fronzoni
Dipartimento di Fisica, Università della Calabria, Rende, Cosenza, Italy
(Received 21 February 1990; revised manuscript received 18 April 1990)

We propose an analog apparatus simulating a standard Josephson junction, which allows easy experimental manipulations and measurements. We center our attention on the onset of chaotic responses, in particular on its dependence on the different physical parameters, and we obtain quite good agreement with other existing data. Great attention is also paid to compare the results with the theoretical threshold of chaos we deduce from Melnikov's method: The agreement is globally as good as possible, taking into account the approximations and the validity of the method; in particular, we obtain a description of the behavior of the threshold for small frequencies, and of the important role played by the dc bias term. We also discuss, both theoretically and experimentally, the case of a Josephson junction to which a periodic modulating term has been added.

I. INTRODUCTION

Considerable effort, both experimental and theoretical, has been devoted to the analysis of the Josephson junction (JJ), especially for what concerns the determination of the onset of chaotic responses (see Refs. 1–10, and references therein). This analysis, in fact, is far from easy, not only for the intrinsic difficulties connected to nonlinear phenomena, but also for the relatively large number of the physical parameters involved, which even makes the comparison difficult between different sets of results available in the literature.

For these reasons it may be useful to resort to an analog simulation by means of a suitable device, prepared in such a way to produce responses obeying the same equation as that describing the JJ. The advantage of this device is the possibility of performing with relative simplicity a large number of observations and measurements, and of directly investigating the dependence of the threshold of chaos on the various physical parameters.

The results obtained in this way will be compared not only with other available data, but also with the theoretical results deduced according to the Melnikov method for the determination of the threshold of chaos[11–15] (see Sec. III). In Sec. II we briefly comment on the validity of this method, discussing why we found it very convenient and instructive to choose Melnikov results as a comparison test for our experimental results.

Taking advantage of the great adaptability and possibilities offered by the analog equipment, we will also investigate the case of a "modulated" JJ, in which a modulating time-periodic term in the effective potential is introduced (Sec. IV).

II. THE EXPERIMENTAL DEVICE AND THEORETICAL APPROACH

Analog simulations of JJ have been obtained by several authors in the past.[3,16–19] In particular, the simulation carried out by D'Humieres *et al.*[3] shows a wide panorama for different values of the control parameters of the system, and it was performed with a phase-locked loop. In our simulations we use the same technique, but with the introduction of some improvements by means of the "minimum components technique," recently developed in our laboratory.[20] Figure 1 shows the scheme of the electronic circuit that we will use (the interested reader can find some detail in the Appendix).

The dynamics of the JJ system is examined, as suggested in Ref. 3, by directly observing the phase-space portraits $(\sin\phi, \dot{\phi})$ on the oscilloscope screen [ϕ being the junction phase, as usual; see Eq. (3) and the Appendix]; then, Poincaré sections are obtained by means of a modulation of a z-axis oscilloscope synchronized to the driving signal.

The threshold of chaos is defined by the value of the ac driving voltage that produces the appearance of a strange attractor in the Poincaré sections; after that, all dynamical transients have disappeared. Due to unavoidable hysteresis effects, one could obtain different thresholds for increasing and decreasing values of the parameters: In our measurements, we always take only the data for increasing driving voltage.

The errors in the determination of the threshold of chaos are produced essentially by three effects: (i) the internal and external electronic fluctuations of the device, which have been reduced using a minimum number of

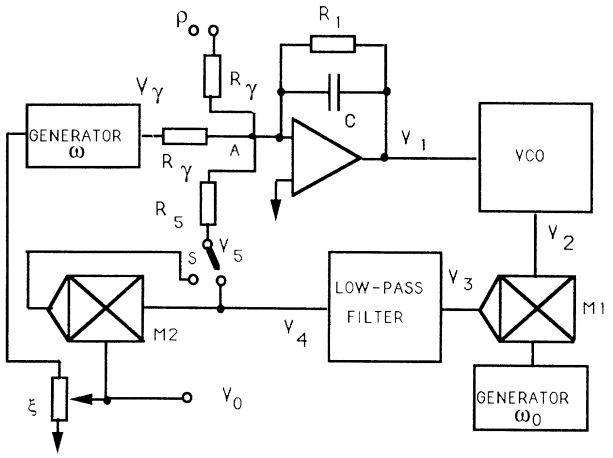

FIG. 1. Scheme of the electronic analog circuit model for the "standard" JJ and the "modulated" JJ.

electronic components and assembling them in only one block, according to our simulation techniques;[20] (ii) thermal drifts of the electronic components (this causes, principally, a drift of the constant dc term which can be easily compensated); (iii) the presence of thin structures close to the boundaries of the ordered and chaotic regions, which makes difficult the precise determination of the threshold (cf. Refs. 2, 3, and 7).

The error bars shown in the experimental measurements are evaluated by a rough standard deviation of the data obtained for each choice of parameters; it can be noted, in fact, that because of the competition of both stochastic and deterministic noise, the statistics are not expected to be strictly Gaussian.

This threshold will be compared with the theoretical value obtained by means of the classical Melnikov method.[11–15] Let us now state Melnikov's results in a convenient form for our purposes. We write the equation describing the problem in the following rather general form [with $\phi=\phi(t)$, $-\pi<\phi<\pi$]:

$$\ddot{\phi}=-\sin\phi+\rho_0+\epsilon F(\phi,\dot{\phi},t)\ , \tag{1}$$

where ρ_0 is the dc component, and F includes all non-Hamiltonian contributions ("damping," ac forcing terms, and possibly other perturbations). The condition for the appearance of the typical "Smale-horseshoe" chaos[10–15] is given by the vanishing of the Melnikov function $M(t_0)$; i.e.,

$$M(t_0)=\int_{-\infty}^{+\infty} dt\,\dot{\phi}_0(t)F(\phi_0(t),\dot{\phi}_0(t),t+t_0)=0\ , \tag{2}$$

where

$$\phi_0=\phi_0(t) \tag{2'}$$

is the homoclinic orbit for the problem (1), evaluated at the Hamiltonian limit $\epsilon=0$.

In the case of the "standard" JJ, which will be considered in Sec. III, Eq. (1) becomes, in dimensionless variables as usual,

$$\ddot{\phi}=-\sin\phi+\rho_0-\delta\dot{\phi}+\gamma\cos\omega t\ , \tag{3}$$

where $\delta=\beta_c^{-1/2}$, β_c being the McCumber parameter, and γ is the amplitude of the ac driving term with normalized frequency ω. We can assume that $\delta,\gamma,\omega>0$.

Being a perturbative approach, Melnikov's method is clearly expected to be valid at the limit $\epsilon\approx 0$, i.e., in the region of nearly vanishing non-Hamiltonian terms. Following an argument in Ref. 9, we can expect that the sufficient conditions ensuring the validity of the method would be the following:

$$\delta\ll\tfrac{1}{4},\quad \rho_0\ll 1/\pi,\quad \gamma\ll 1/\pi\ . \tag{4}$$

We will respect these prescriptions in part, but in part we will operate at the extreme-limit case (e.g., we will set, for operational convenience, $\delta=0.25$). On the other hand, a tentative extension of the procedure beyond the range of strictly small values of the perturbing parameters might provide some instructive information (see, e.g., Refs. 13 and 14 for a discussion and some related remarks. Notice also that the Melnikov method actually deals with the occurrence of transverse homoclinic points, which are to be considered as "precursors of chaos;" one can say, in general, that the actual threshold becomes visible a little bit over the Melnikov indications).

Many other ways (or "scenarios"), different from or even in competition with the Melnikov approach, have been proposed as routes leading to chaos; however, in this paper we will refer exclusively to Melnikov's results for two essential reasons: (i) From the experimental point of view, we detect chaos starting from a regular phase-space trajectory, near the separatrix (cf. Ref. 3); by increasing the driving voltage we produce the perturbation which breaks the homoclinic loop, as prescribed by Melnikov's technique. (ii) From the theoretical point of view, the Melnikov method is one of the (few) analytical methods suitable for describing very different situations and (at least, in principle) several intervals of variations of the physical parameters: This makes it a very useful "reference guide" for testing experimental results.

In view of the above remarks, it is clear that we cannot hope that the agreement of theoretical and experimental results will be excellent; rather, we will consider it a good result if the experimental curves exhibit a global qualitative behavior roughly "similar" to the theoretical curves, and we expect discrepancies to increase as the perturbations increase in importance.

III. "STANDARD" JJ: EXPERIMENTAL AND THEORETICAL RESULTS

We devote this section to the case of the "standard" JJ, which is described by Eq. (3). First of all, let us recall that in the case of no dc bias, i.e., $\rho_0=0$, there are two homoclinic orbits [Eq. (2')] given explicitly by (see, e.g., Ref. 14)

$$\phi_0(t)=\pm(4\arctan e^t-\pi),\quad \dot{\phi}_0(t)=\pm 2\,\mathrm{sech}\,t\ , \tag{5}$$

and that, in this case, the above condition (2) for the appearance of chaotic responses becomes, as is well known[14] [independently of the $\pm$ sign in (5)],

$$\frac{\gamma}{\delta} \geq \frac{4}{\pi}\cosh\frac{\omega\pi}{2} \equiv R_0(\omega) , \tag{6}$$

where we have introduced for convenience the "Melnikov ratio" $R_0 = R_0(\omega)$. This condition, however, does not completely agree with the available experimental results [see, e.g., in Fig. 2, curves (a) and (b), which represent the rough envelope of the chaotic region, taken from Ref. 3 and Refs. 2 and 10, respectively], especially for relatively small ω; in particular, Eq. (6) does not show any minimum point for the threshold, in contrast with experiments. The low-frequency behavior of the threshold has been the object of another previous analysis[9]: it has been shown through digital simulations that there is a narrow region of chaos, which is accurately described by Melnikov's result, while the higher onset typically observed in simulations is seen as an effect associated with a saddle-node bifurcation, unrelated to the Melnikov picture. The very simple explanation we are considering here, based on Melnikov's idea, may be the unavoidable presence of some very small dc term $\rho_0 \neq 0$. It has been show,[21] in fact, that this term drastically changes precisely the low-frequency behavior of the threshold for chaos: In Fig. 2, the other three curves give the theoretical values we obtain from condition (2) for the threshold, with different values of ρ_0 as indicated. It can be a remarkable fact that there is qualitative agreement of these theoretical results with previous experiments and, in particular, the correct position of the minimum of the threshold line $R = R(\omega,\rho_0)$ at $\omega \approx 0.6$ (changing ρ_0 does not sensibly change this position).

Note also that when $\rho_0 \neq 0$, Melnikov's integral (2) cannot be evaluated analytically, but precise numerical calculations are possible[21] even without the explicit expression of the homoclinic orbit for this case. Moreover, in particular, it can be proved by means of general arguments based on Melnikov's condition (2) that if $\rho_0 \neq 0$, and if the critical points are hyperbolic, the threshold function R behaves near $\omega = 0$ as $1/\omega$ (obviously, in the extreme range $(0 \approx \omega < \delta)$, one also has to take into account the condition $\gamma < 1$, which guarantees at the static limit the permanence of critical homoclinic points).

All of the above discussion shows the interest and the relevance of the dc term ρ_0 in the JJ. We now present in Fig. 3 the experimental results we obtained by means of the analog device described in Sec. II. Keeping $\delta = 0.25$ fixed, we plot as a function of ω the threshold values for the appearance of chaos of the amplitude γ in the two

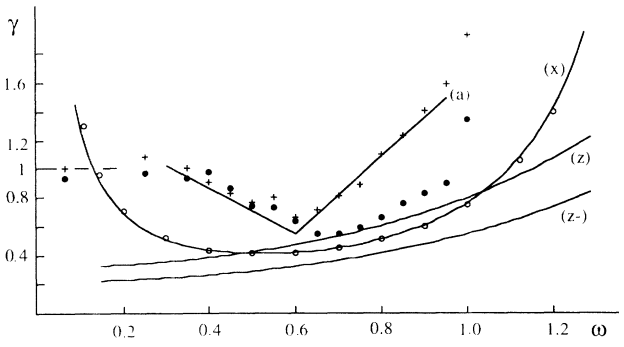

FIG. 3. Threshold values of the amplitude γ for the appearance of chaos. Curve (a) is the same as (a) in Fig. 2; small crosses (+) and solid circles (●) give the experimental values obtained by means of our analog simulation, respectively, with $\rho_0 = 0$ and $\rho_0 = 0.1$. Open circles (○) are the theoretical values we deduce by means of Melnikov's method with $\rho_0 = 0.1$, and curve (x) is the theoretical threshold [Eq. (9)] obtained from the modified potential (8). Finally, (z) is the plot of the quantity $R_0(\omega)\delta$, with R_0 given by Eq. (6), and (z^-) is the lower threshold $R_-(\omega,\rho_0)\delta$, obtained from the approximate expression (11) with $\rho_0 = 0.1$. In all of the data, we assume that $\delta = 0.25$.

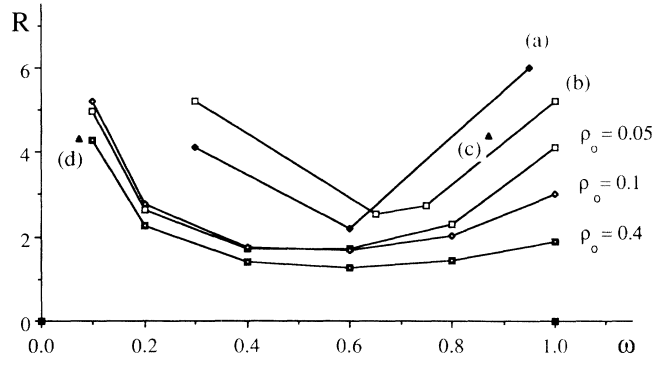

FIG. 2. Threshold for chaos in a JJ. Chaos appears if $\gamma/\delta \geq R$. Curves (a) and (b) are rough boundary lines separating chaotic from regular regions taken from Ref. 3 and Refs. 2 and 10, respectively. Points (c) and (d) are taken from Ref. 4 with $\rho_0 \approx 0.05$, and Ref. 8 with $\rho_0 \approx 0.1$, respectively. The other lines show the theoretical values we obtained from the Melnikov condition for three different values of the dc bias ρ_0 as indicated.

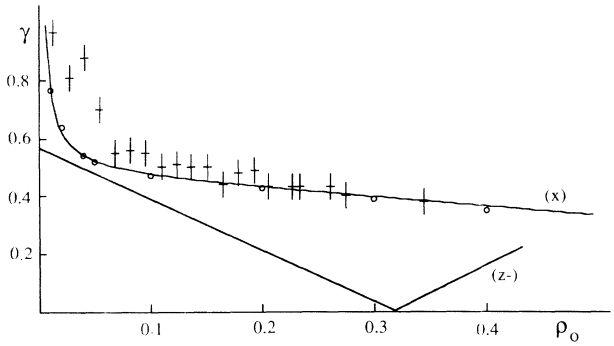

FIG. 4. Threshold values of the amplitude γ for the appearance of chaos vs the dc term ρ_0, for fixed $\delta = 0.25$ and $\omega = 0.75$. The set of values we obtained by means of the analog simulation are compared with the theoretical results from the Melnikov condition (○). Curve (x) is deduced theoretically [Eq. (9)] from the modified potential (8). Finally, curve (z^-) is the lower threshold given by the approximate formula (11).

cases: $\rho_0=0$, small crosses, and $\rho_0=0.1$, closed circles (experimental errors are not shown here, for simplicity; see, however, Figs. 4 and 5). In Fig. 3, curve (a) is the same as curve (a) in Fig. 2 and is drawn here for reference, in order to show the very good agreement of our data with other experimental results. These data are also compared with the values (open circles along the curve (x) in the same Fig. 3) that we numerically deduced from the Melnikov condition, with $\rho_0=0.1$. Finally, curve (z) is the plot of the function $R_0(\omega)\delta$, with R_0 given by Eq. (6). The above analysis is confirmed by this set of results.

In addition, let us mention the very critical behavior of the threshold for $\rho_0\approx 0$, as discussed elsewhere.[21-23] This depends on the fact that the linear term $-\rho_0\phi$ in the potential corresponding to Eq. (1),

$$V(\rho_0,\phi)=-\cos\phi-\rho_0\phi \tag{7}$$

not only breaks the reflection symmetry of the pendulum-like potential $V(0,\phi)$, but also drastically changes the global behavior of the homoclinic orbits: For example, if $\rho_0=0$, these orbits are *odd* functions of time, whereas they become *even* functions if $\rho_0\neq 0$; thus we can say that the global properties of the potential $V(0,\phi)$ are "unstable" against the perturbation $-\rho_0\phi$.

In order to complete our analysis, we also studied the dependence on ρ_0 of the threshold: Figure 4 shows the results obtained by means of the analog apparatus, and the small circles are the theoretical values deduced from the Melnikov condition, with fixed $\omega=0.75$, and $\delta=0.25$. The agreement is even better than the agreement in Figs. 2 and 3.

As remarked above, analytical calculations are not possible in the Melnikov integral (2) if $\rho_0\neq 0$; it may be interesting to observe, however, that by substituting the JJ potential (7) with the following one [very similar to (7)],

$$V(\rho_0,\phi)=-\cos\phi-\pi\rho_0\sin\frac{\phi}{2}\quad(-\pi<\phi<\pi)\ , \tag{8}$$

the Melnikov integral can then be explicitly evaluated to get the following condition for chaos[22]:

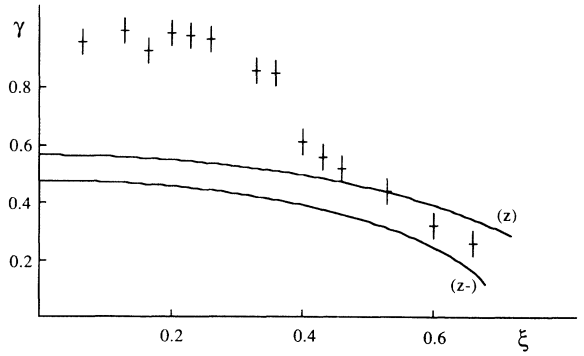

FIG. 5. Experimental (via analog simulation) and theoretical thresholds for chaos, in the presence of modulation vs the modulating amplitude ξ. Curves (z) and (z^-) are deduced from formula (14), with $\rho_0=0$ and $\rho_0=0.05$, respectively, and $\theta=0$. The other parameters are $\delta=0.25$ and $\omega=0.75$.

$$\gamma\geq 4\frac{\delta}{\pi}\cosh\left[\frac{\omega\pi}{2\nu}\right]\frac{\nu-\pi\rho_0(\lambda/4)}{|\sin(\omega\lambda/\nu)|}\ , \tag{9}$$

where

$$\nu=\left[1-\pi\frac{\rho_0}{4}\right]^{1/2}\ , \tag{10}$$

$$\lambda=\ln(1+\nu)-\tfrac{1}{2}\ln\pi\frac{\rho_0}{4} \tag{10'}$$

(which confirms, in particular, the expected very critical limit $\rho_0\approx 0$). The curves denoted by (x) in Figs. 3 and 4 are just the right-hand side of Eq. (9), plotted, respectively, as a function of ω, with $\rho_0=0.1$, and of ρ_0, with $\omega=0.75$. The perfect agreement of these curves with the numerical results (open circles) obtained for the JJ potential (7) shows that the above modified potential (8) really provides a very good description of the JJ potential, with the advantage of allowing analytic calculations.

To conclude this section, let us briefly comment on an approximate method,[5,6,9,10] which has been used for dealing with the dc term ρ_0, and on its validity. This method amounts to moving the term ρ_0 from the Hamiltonian into the perturbative part ϵF of the equation (1): As a consequence, its effect in the Melnikov integral (2) simply amounts to a perturbation of the homoclinic orbit in the form (5). According to this approach, the Melnikov condition (2) explicitly[5,6,9,10] becomes

$$\gamma\geq\delta R_0(\omega)\left|1\pm\frac{\pi\rho_0}{4\delta}\right|=\delta R_\pm(\omega,\rho_0)\ , \tag{11}$$

where $R_0(\omega)$ is given in (6), and the "double" sign of $\pm$ depends on the sign in (5). It can be remarked that this "doubling" of the threshold would indicate that the appearance of chaos may be favored or not, depending on the relative signs of ρ_0 and $\dot\phi_0$; but clearly, when averaged on several cycles, the mean effect will be that of choosing the lower curve as the actual threshold. In Figs. 3 and 4, the curve (z^-) is precisely this threshold. From these figures, we can see that the method described here provides a fairly good approximation when $\rho_0\approx 0.05$–0.1 and $\omega\gtrsim 0.5$.

IV. "MODULATED" JJ

Let us now introduce in the JJ a modulating term with (small) amplitude ξ and frequency Ω, according to the following equation:

$$\ddot\phi=-[1+\xi\cos(\Omega t+\theta)]\sin\phi+\rho_0-\delta\dot\phi+\gamma\cos\omega t\ . \tag{12}$$

Again, the Melnikov method can be applied: In particular, if $\rho_0=0$, the integral (2) can be evaluated to give the following condition:

$$M(t_0)=-8\delta\pm 2\pi\gamma\,\mathrm{sech}\frac{\omega\pi}{2}\cos\omega t_0 + 2\pi\xi\Omega^2\,\mathrm{csch}\frac{\Omega\pi}{2}\sin(\Omega t_0+\theta)=0\ . \tag{13}$$

A rough result that can be immediately deduced from

(13) is that a sufficient condition—independent of the ambiguity in the $\pm$ sign and of the phase difference θ—for the chaos does *not* appear (we can assume here that $\xi>0$) is

$$\gamma \operatorname{sech}\frac{\omega\pi}{2}+\xi\Omega^2\operatorname{csch}\frac{\Omega\pi}{2}<\frac{4\delta}{\pi} .$$

Again, the $\pm$ sign in (13) originates from the double sign in the homoclinic orbit ϕ_0 (5); it is easy to verify that changing this sign is the same as changing the sign of ξ, or that of θ. We can say that the presence of the modulation introduces an asymmetry between the orbit with $\dot{\phi}_0>0$ and that with $\dot{\phi}_0<0$, but we can expect that the mean effect will be that of lowering the actual threshold of chaos.

In order to get a more detailed and easy analysis of the situation, let us choose $\omega=\Omega$ from now on. In Fig. 5, the experimental results we obtained for the threshold values of γ, having fixed $\rho_0=0$ and $\theta=0$, are given as a function of the modulation amplitude ξ; in the same Fig. 5, curve (z) is the theoretical threshold deduced from (13). The explicit expression of this curve can be directly obtained from (14) below putting $\rho_0=\theta=0$. Once again, we obtain a very rough qualitative agreement; on the other hand, the presence of a further perturbation term would produce a condition of the following type [more stringent than in (4)] for the validity of the approach:

$$|\gamma|+|\xi|\ll 1/\pi ,$$

and this clearly makes its accuracy even more problematic.

We see that the global effect of the modulation is that of lowering the threshold, i.e., of favoring chaos. Interestingly, this result may be compared with the situation considered in Ref. 24, where it is shown both numerically and theoretically that a resonant modulation in a Duffing-Holmes oscillator produces, on the contrary, a suppression of chaos. The opposite effects of the modulation in these two cases actually depends on the different form of the potential functions and the homoclinic orbits involved, which produce different types of contributions in the Melnikov function.[25] It can be noted that if $\rho_0\neq 0$, the JJ potential (7) becomes somewhat "similar" to the Duffing-Holmes potential, and that the more the ρ_0 is large, the more this similarity looks true. Actually, neither ρ_0 nor ξ can be chosen to be too large in our case (preserving the existence of critical points in the potential gets the condition $|\rho_0|+|\xi|+|\gamma|<1$); so we can expect that including modulation in the presence of $\rho_0\neq 0$ should produce small changes in the threshold of chaos. Numerical calculations based again on the Melnikov technique show, in fact, that for $\rho_0\approx 0.4$, $\omega=0.75$, and $\xi\approx 0.4$, one should expect an increase (very small, in fact) of the threshold value γ of the order $\Delta\gamma\approx 0.06$. If ρ_0 is small, this effect is completely negligible; then, let us finally write down, for completeness, the theoretical expression for the threshold of chaos we would obtain by treating this term $\rho_0\neq 0$ according to the approximate method sketched at the end of Sec. III (in the hypothesis $\xi\omega^2\leq|4\delta/\pi-\rho_0|$):

$$\gamma\geq\delta R_0(\omega)\left\{\frac{-\pi\xi\omega^2}{4\delta}\operatorname{csch}\frac{\omega\pi}{2}\sin\theta+\left[\left[1-\frac{\pi\rho_0}{4\delta}\right]^2-\left[\frac{\pi\xi\omega^2}{4\delta}\operatorname{csch}\frac{\omega\pi}{2}\cos\theta\right]^2\right]^{1/2}\right\} , \quad (14)$$

where $R_0(\omega)$ is the usual expression (6). In Fig. 5, curve (z^-) shows this threshold for $\theta=0$ and $\rho_0=0.05$.

In conclusion, we can say that the analog device presented in this paper reveals to be a useful tool. The agreement with other existing data is very good; also, the comparison with theoretical results deduced via the Melnikov method appears, in general, to be rather satisfying and interesting.

APPENDIX: THE ANALOG DEVICE

The scheme of the circuit is in Fig. 1: With the switch S in the position shown, the sum of the currents at the point A gives

$$\frac{V_5}{R_5}+\frac{V_1}{R_1}+\frac{V_\gamma}{R_\gamma}+C\dot{V}_1=0 , \quad (A1)$$

where V_γ is the driving voltage, produced by a generator applied to the input. The phase of the signal V_2 at the output of the voltage-controlled oscillator (VCO) is driven by the voltage V_1 according to the relation $\dot{\phi}=kV_1$, where k is the VCO frequency-modulation coefficient. If ω_0 is the VCO frequency, then $V_2=\sin(\omega_0 t+\phi)$. The generator connected to the Miller multiplier $M1$ is tuned at the same frequency, so that at the output of $M1$ we obtain

$$V_3=\sin(\omega_0 t+\phi)\cos\omega_0 t=\tfrac{1}{2}[\sin\phi+\sin(2\omega_0 t+\phi)] . \quad (A2)$$

The frequency cutoff of the low-pass filter is chosen in such a way as to exclude the component at frequency $2\omega_0$ (in our case, $\omega_0=628$ kc/s). Then $V_5=\frac{1}{2}\sin\phi$, and the Eq. (A1) reads as

$$\frac{\sin\phi}{2R_5}+\frac{\dot{\phi}}{kR_1}+\frac{V_\gamma}{R_\gamma}+\frac{C}{k}\ddot{\phi}=0 , \quad (A3)$$

which is the same as (3), once written in dimensionless variables and taking into account that

$$V_\gamma=-(\gamma\cos\omega t+\rho_0)R_\gamma/2R_5 . \quad (A4)$$

In order to introduce a modulation, we apply the voltage V_4 to the input of a second multiplier AD 534, and the switch S is turned to the left position (see Fig. 1). A fraction V_m of the ac voltage of the forcing generator is added to a dc voltage V_0 and connected to the other input of the multiplier $M2$. In this way, the reaction volt-

age is

$$V_5 = (V_0 + V_m \cos\omega t)\sin\phi$$
$$= V_0(1 + \xi \cos\omega t)\sin\phi \ , \qquad \text{(A5)}$$

where $\xi = V_m / V_0$. This ensures, in particular, the equality of the frequencies and phases of both components (driving and modulating) during the experiments. Once written in dimensionless variables, the equation of the circuit now becomes Eq. (12), with $\omega = \Omega$ and $\theta = 0$.

[1]B. A. Huberman, J. P. Crutchfield, and N. Packard, Appl. Phys. Lett. **37**, 750 (1980).

[2]N. F. Pedersen and A. Davidson, Appl. Phys. Lett. **39**, 830 (1981).

[3]D. D'Humieres, M. R. Beasley, B. A. Huberman, and A. Libchaber, Phys. Rev. A **26**, 3483 (1982).

[4]M. Cirillo and N. F. Pedersen, Phys. Lett. A **90**, 150 (1982).

[5]Z. D. Genchev, Z. G. Ivanov, and B. N. Todorov, IEEE Trans. Circuits Syst. **CAS-30**, 633 (1983).

[6]F. M. A. Salam and S. S. Sastry, IEEE Trans. Circuits Syst. **CAS-32**, 784 (1985).

[7]R. L. Kautz and R. Monaco, J. Appl. Phys. **57**, 875 (1985).

[8]C. Vanneste, C. C. Chi, and D. C. Cronemeyer, Phys. Rev. B **32**, 4796 (1985).

[9]R. L. Kautz and J. C. Macfarlane, Phys. Rev. A **33**, 498 (1986).

[10]M. Bartuccelli, P. L. Christiansen, N. F. Pedersen, and M. P. Soerensen, Phys. Rev. B **33**, 4686 (1986).

[11]V. K. Melnikov, Trans. Moscow Math. Soc. **12**, 1 (1963).

[12]V. I. Arnold, Sov. Math. Dokl. **5**, 581 (1964).

[13]A. J. Lichtenberg and M. A. Lieberman, *Regular and Stochastic Motion* (Springer, New York, 1983).

[14]J. Guckenheimer and P. J. Holmes, *Nonlinear Oscillations, Dynamical Systems, and Bifurcations of Vector Fields* (Springer, New York, 1983).

[15]S. Wiggins, *Global Bifurcations and Chaos* (Springer, New York, 1988).

[16]C. A. Hamilton, Rev. Sci. Instrum. **43**, 445 (1972).

[17]C. K. Bak and N. F. Pedersen, Appl. Phys. Lett. **22**, 149 (1973).

[18]J. H. Magerlein, Rev. Sci. Instrum. **49**, 486 (1978).

[19]A. Yagi and I. Kurosawa, Rev. Sci. Instrum. **51**, 14 (1980).

[20]L. Fronzoni, in *Noise in Nonlinear Dynamical Systems* edited by by F. Moss and P. V. E. McClintock (Cambridge University Press, Cambridge, 1989), Vol. 3, p. 222.

[21]G. Cicogna, Phys. Lett. A **121**, 403 (1987).

[22]G. Cicogna, Phys. Lett. A **131**, 98 (1988).

[23]G. Cicogna, Acta Mech. **76**, 189 (1989).

[24]R. Lima and M. Pettini, Phys. Rev. A **41**, 726 (1990).

[25]G. Cicogna, Nuovo Cimento B (to be published).